International Journal of Applied Electromagnetics and Mechanics 33 (2010) 87–93
DOI 10.3233/JAE-2010-1100
IOS Press

Modeling of giant magnetostrictive actuator based on hysteretic nonlinear theory

Zhi-Wen Zhu*, Yue Liu, Jia Xu and Hong-Li Wang
School of Mechanical Engineering, Tianjin University, 92 Weijin Road, Tianjin 300072, P.R. China

Abstract. In this paper, a kind of giant magnetostrictive actuator (GMA) model based on hysteretic nonlinear theory was developed. Nonlinear difference item was introduced to interpret the hysteresis phenomenon of GMA. The coupling relationship between magnetic field intensity and frequency was obtained in stepwise multiple regression method to describe the driftage of strain curve. Based on above, the final relationship among strain, magnetic field intensity and frequency was set up. The result of significance test shows that the effects of all of the items in the final model are remarkable, which means that the model can describe the characteristics of GMA in different frequencies well. The new GMA model broadens the region of controlling frequency, and is easy to be analyzed in theory, which is helpful to vibration control.

1. Introduction

Giant magnetostrictive material (GMM) has many characteristics such as giant strain, rapid response, and excellent control resolution, based on which the giant magnetostrictive actuator (GMA) used in mechanical system can be designed to control vibration accurately. There are many physical models of GMM [1–4]. D.C. Jiles and D.L. Atherton set up the GMM model based on electromagnetics theory [1]. J.B. Restorff developed a Preisach model in Terfenol-D [2]. G.P. Carman studied nonlinear constitutive relations for magnetostrictive materials [3]. F.T. Calkins developed a hysteresis model for magnetostrictive transducers based on energy [4]. For the hysteresis characteristics of GMM, most of the GMM models were shown as equations with subsection function or double integral function and were hard to be analysed in theory. Usually, research results could only be obtained by numerical or experiment method [5–8]. In this paper, hysteretic nonlinear theory was introduced to develop a new kind of continuous GMA strain-magnetic field intensity-frequency model, in which the driftage of strain curve caused by the variation of frequency was described.

2. Hysteresis model of GMM

The curve of strain-magnetic field intensity (MFI) of GMM was shown in Fig. 1. The curve is a hysteresis loop. Based on Van de Pol equation, the nonlinear hysteresis model of GMM in constant frequency can be shown as follows:

$$\lambda = \alpha H_0 + \beta H - \gamma H^2 + \eta H^3 + \mu(\upsilon H - H^2)\dot{H} = \lambda_1 + \lambda_2 \tag{1}$$

*Corresponding author: Zhi-Wen Zhu, School of Mechanical Engineering, Tianjin University. Tel.: +86 22 27401981; Fax: +86 22 27401981; E-mail: gclx309@yahoo.com.cn.

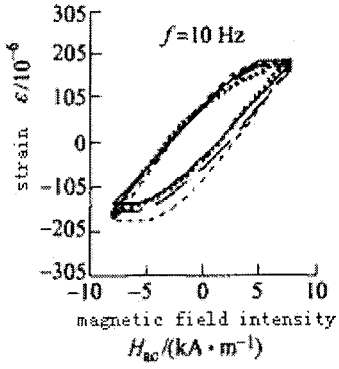

Fig. 1. The curve of strain and magnetic field intensity.

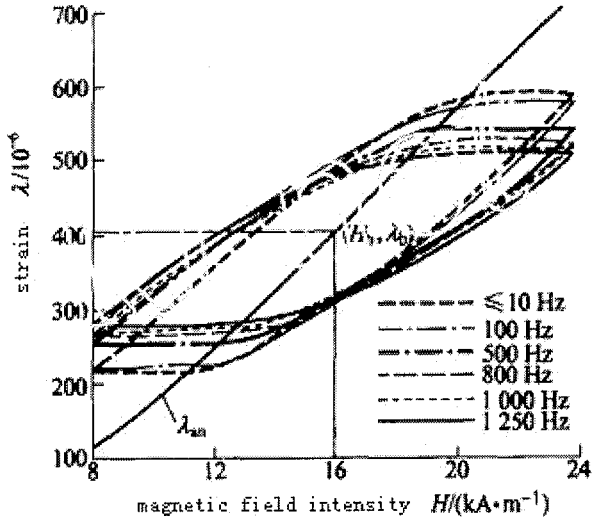

Fig. 2. The curves of strain in different frequencies.

where λ is strain caused by magnetostriction, H_0 is the intensity of bias magnetic field, $H_0 = 0$ when bias magnetic field is absent, H is magnetic field intensity, α, β, γ, η, μ, υ are coefficients. $\lambda_1 = \alpha H_0 + \beta H - \gamma H^2 + \eta H^3$ is skeleton curve of the strain-MFI curve, $\lambda_2 = \mu(\upsilon H - H^2)\dot{H}$ shows difference between the skeleton curve and the real curve.

The variation of frequency will influence strain curve of GMM, which was named driftage phenomena and shown in Fig. 2. It causes the error in dynamical analysis and control. For finding the relationship among strain, magnetic field intensity and frequency, basic items in GMM model should be determined before the data mining method was applied. Supposing that all the coupling items about H and f will appear in the model, the basic model of λ where the variation of frequency was considered can be shown as follows:

$$\begin{aligned}\lambda = {} & \lambda_0 + a_0 f + a_1 H - a_2 H^2 + a_3 H^3 + a_4 H\dot{H} + a_5 H^2\dot{H} + a_6 Hf + a_7 H^2 f + a_8 H^3 f \\ & + a_9 H\dot{H}f + a_{10} H^2\dot{H}f + a_{11} Hf^2 + a_{12} H^2 f^2 + a_{13} H^3 f^2 + a_{14} H\dot{H}f^2 \\ & + a_{15} H^2\dot{H}f^2 + a_{16} Hf^3 + a_{17} H^2 f^3 + a_{18} H^3 f^3 + a_{19} H\dot{H}f^3 + a_{20} H^2\dot{H}f^3\end{aligned} \tag{2}$$

Table 1
Fitting result of all of the items

	Estimate	Std.Error	t value	Pr(>|t|)
f	3.41E+02	3.12E+01	10.947	<2.00E-16
H	7.50E-02	2.04E-02	3.674	0.000443
H^2	-5.68E-05	8.25E-06	-6.881	1.47E-09
H^3	-1.49E+01	7.05E+00	-2.119	0.037378
$H\dot{H}$	-9.35E+00	1.40E+01	-0.666	0.507134
$H^2\dot{H}$	4.43E-01	6.45E-01	0.687	0.49429
Hf	-5.44E-03	1.54E-02	-0.353	0.725181
H^2f	-3.19E-05	4.68E-05	-0.682	0.49761
H^3f	7.83E-08	4.24E-08	1.846	0.068747
$H\dot{H}f$	3.92E-02	2.00E-02	1.958	0.053857
$H^2\dot{H}f$	-1.92E-03	8.97E-04	-2.141	0.035509
Hf^2	-2.91E-05	1.20E-05	-2.428	0.017568
H^2f^2	1.32E-07	4.82E-08	2.746	0.007534
H^3f^2	-1.52E-10	7.35E-11	-2.07	0.041827
$H\dot{H}f^2$	4.76E-06	8.93E-06	0.533	0.59544
$H^2\dot{H}f^2$	NA	NA	NA	NA
Hf^3	1.88E-08	1.10E-08	1.707	0.091868
H^2f^3	-7.69E-11	3.55E-11	-2.165	0.033565
H^3f^3	8.18E-14	3.95E-14	2.069	0.041991
$H\dot{H}f^3$	-1.02E-08	1.34E-08	-0.76	0.449348
$H^2\dot{H}f^3$	3.77E-10	5.80E-10	0.65	0.517485

where $\lambda_0 = \lambda_0(H_0)$ is relative to bias magnetic field intensity H_0. Obviously, Eq. (2) is very complex, and there must be some items whose effects are not remarkable in the basic model. In this paper, stepwise multiple regression method was applied in finding the relationship between H and f. Reading experimental data from Fig. 2 and regarding the items above as independent variables, the items whose effects are not remarkable in the basic model were eliminated step by step according to Akaike Information Criterion (AIC). Fitting results of all of the items in multiple nonlinear regression method were shown in Table 1, and analysis results of fitting variance of possible items in multiple nonlinear regression method were shown in Table 2, where Std.Error is Standard Error, Pr is Probability, Df is degree of freedom, RSS is regression sum of squares.

Choosing the items whose Pr values are little from Table 3, we obtained the relationship among strain, MFI and frequency as follows:

$$\lambda = \lambda_0 + b_0 f + b_1 H + b_2 H^2 + b_3 H^3 + b_4 H f^2 + b_5 H^2 f + b_6 H\dot{H} + b_7 H^2\dot{H} \tag{3}$$

To Eq. (3), residual sum of squares is 4.671, the corresponding degree of freedom is 82, coefficient of determination R^2 is 0.9979, adjusted coefficient of determination is 0.9976; F statistic is 3043, the corresponding degrees of freedom are 13 and 82, concomitant probability $p < 2.2 \times 10^{-16}$, so the effects of all of the items in Eq. (3) are remarkable. It means that the equation can describe the strain-MFI curves of GMM in different frequencies well.

Equation (3) only shows that the items: f, H, H^2, H^3, Hf^2, H^2f, $H\dot{H}$, $H^2\dot{H}$ should appear in the final model, while the coefficient b_i ($i = 0\sim7$) must be obtained in fitting method. We assumed that

Table 2
Analysis results of fitting variance of possible items

	Df	Sum of Sq	RSS	AIC
Hf	1	2.88	1759.17	317.19
$H\dot{H}f^2$	1	6.57	1762.86	317.39
$H^2\dot{H}f^3$	1	9.77	1766.06	317.57
$H\dot{H}$	1	10.26	1766.56	317.59
H^2f	1	10.73	1767.03	317.62
$H^2\dot{H}$	1	10.9	1767.19	317.63
$H\dot{H}f^3$	1	13.36	1769.66	317.76
f	1	32.54	1756.29	319.03
Hf^3	1	67.35	1823.65	320.65
H^3f	1	78.77	1835.07	321.25
$H\dot{H}f$	1	88.63	1844.92	321.76
H^3f^3	1	98.88	1855.17	322.29
H^3f^2	1	99.04	1855.34	322.3
H	1	103.74	1860.03	322.54
$H^2\dot{H}f$	1	105.9	1862.19	322.66
H^2f^3	1	108.27	1864.56	322.78
Hf^2	1	136.18	1892.47	324.2
H^2f^2	1	174.21	1930.5	326.11
H^2	1	311.87	2068.17	332.73
H^3	1	1094.18	2850.47	363.53

Table 3
Result of significance test of items

	Estimate	Std.Error	t value	Pr(>|t|)	Signif. codes
f	3.25E+02	1.07E+01	30.298	<2.00E-16	***
H^2	8.87E-02	3.58E-03	24.776	<2.00E-16	***
H^3	-6.02E-05	4.08E-06	-14.755	<2.00E-16	***
H	-1.95E+01	1.31E+00	-14.91	<2.00E-16	***
H^2f	-5.23E-05	1.28E-05	-4.103	9.58E-05	***
H^3f	8.06E-08	2.70E-08	2.981	0.003777	**
$H\dot{H}$	2.99E-02	4.13E-03	7.227	2.32E-10	***
$H^2\dot{H}$	-1.36E-03	1.91E-04	-7.108	3.95E-10	***
Hf^2	-2.35E-05	5.95E-06	-3.94	0.00017	***
H^2f^2	1.24E-07	3.97E-08	3.134	0.002396	**
H^3f^2	-1.35E-10	6.00E-11	-2.256	0.026741	*
Hf^3	1.04E-08	3.08E-09	3.384	0.001097	**
H^2f^3	-5.66E-11	2.05E-11	-2.765	0.007029	**
H^3f^3	6.61E-14	3.09E-14	2.141	0.035252	*

Eq. (3) should be similar to Eq. (1) since Eq. (3) shows hysteresis loops in Fig. 2. Thus, the final model should be shown as follows:

$$\lambda = \lambda_0 + c_0 f + c_1 H(1 + c_2 f^2) - c_3 H^2(1 + c_4 f) + c_5 H^3 + c_6(c_7 H - H^2)\dot{H} \tag{4}$$

Comparing Eqs (1) and (4), we obtained

$$\begin{cases} \lambda_1 = \lambda_0 + c_0 f + c_1 H(1 + c_2 f^2) - c_3 H^2(1 + c_4 f) + c_5 H^3 \\ \lambda_2 = c_6(c_7 H - H^2)\dot{H} \end{cases} \tag{5}$$

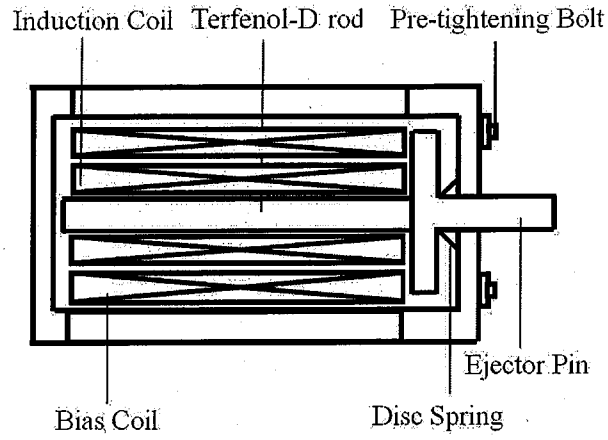

Fig. 3. The structure of GMA.

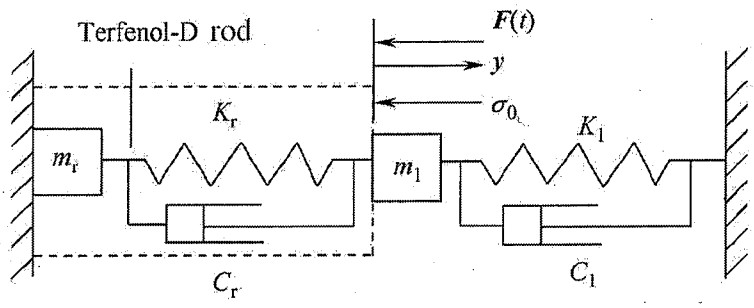

Fig. 4. The equivalent mechanical model of GMA driving system.

and

$$\alpha = (\lambda_0 + c_0 f)/H_0, \quad \beta = c_1(1 + c_2 f^2), \quad \gamma = c_3(1 + c_4 f), \quad \eta = c_5, \quad \mu = c_6, \quad \upsilon = c_7$$

From Fig. 2, we can see that λ_2, which is difference between the skeleton curve and the real curve, hardly varies with frequency, while λ_1, which is skeleton curve of the strain-MFI curve, varies with frequency f of magnetic field obviously. Equations (5) interpreted the phenomena since only λ_1 includes f. It means that the final model (4) is credible.

3. Dynamic model of GMA and experiment

The typical structure of GMA was shown in Fig. 3, and the equivalent mechanical model of GMA driving system was shown in Fig. 4. The mechanical model of GMA can be shown as follows:

$$\varepsilon = \sigma/E + \lambda - (C_r/E)\dot{\varepsilon} - \rho l_r^2 \ddot{\varepsilon}/(3E) \tag{6}$$

where σ is stress, E is Young's elastic modulus, C_r is damping of GMA, ρ is density of GMM, l_r is length of Terfenol-D rod.

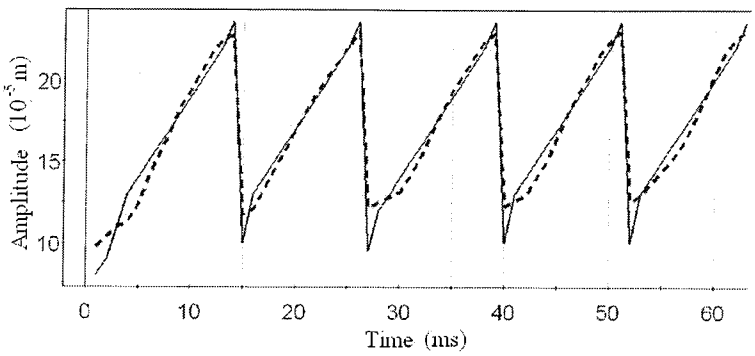

Fig. 5. experimental and numerical result of GMA when f = 80Hz.

Considering $F = \sigma A_r = -(m_1\ddot{y} + c_1\dot{y} + k_1 y)$ and $y = \varepsilon l_r$, Eq. (6) can be rewritten as follows:

$$m_Z\ddot{\varepsilon} + c_Z\dot{\varepsilon} + k_Z\varepsilon = \frac{A_r E}{l_r}\lambda \tag{7}$$

where $m_Z = \frac{m_r}{3} + m_1$, $c_Z = \frac{A_r C_r}{l_r} + c_1$, $k_Z = \frac{A_r E}{l_r} + k_1$, m_r is mass of Terfenol-D rod, m_1 is equivalent mass of load, A_r is cross sectional area of Terfenol-D rod, C_1 is equivalent damping of load, k_1 is equivalent stiffness of load, λ is determined by Eq. (4).

To alternating electromagnetic field in constant frequency, $H = \bar{H}\cos\omega t$, where $\bar{H}$ is the amplitude value of alternating electromagnetic field, $\omega = 2\pi f$. From Eqs (4) and (7), we can obtained:

$$\begin{aligned} m_Z\ddot{\varepsilon} + c_Z\dot{\varepsilon} + k_Z\varepsilon = \frac{A_r E}{l_r}[&\lambda_0 + c_0 f + c_1(1 + c_2 f^2)\bar{H}\cos\omega t - c_3(1 + c_4 f)\bar{H}^2\cos^2\omega t \\ &+ c_5\bar{H}^3\cos^3\omega t - c_6(c_7\bar{H}\cos\omega t - \bar{H}^2\cos^2\omega t)\bar{H}\omega\sin\omega t] \end{aligned} \tag{8}$$

The solution of Eq. (8) is

$$\varepsilon = \varepsilon_0 + \varepsilon_1\cos\omega t + \varepsilon_2\cos 2\omega t + \varepsilon_3\cos 3\omega t + s_4\sin\omega t + \varepsilon_5\sin 2\omega t + \varepsilon_6\sin 3\omega t \tag{9}$$

where $\varepsilon_0 = \frac{A_r E}{k_Z l_r}[\lambda_0 + c_0 f - \frac{1}{2}c_3(1 + c_4 f)\bar{H}^2]$, $\varepsilon_1 = \frac{A_r E}{m_Z l_r \bar{\omega}}[c_1(1 + c_2 f^2)\bar{H} + \frac{3}{4}c_5\bar{H}^3]$, $\varepsilon_2 = -\frac{A_r E}{2m_Z l_r \bar{\omega}}c_3(1 + c_4 f)\bar{H}^2$, $\varepsilon_3 = \frac{A_r E}{4m_Z l_r \bar{\omega}}c_5\bar{H}^3$, $\varepsilon_4 = \frac{A_r E}{4m_Z l_r \bar{\omega}}c_6\bar{H}^3\omega$, $\varepsilon_5 = -\frac{A_r E}{2m_Z l_r \bar{\omega}}c_6 c_7\bar{H}^2\omega$, $\varepsilon_6 = \varepsilon_4$, $\bar{\omega} = \sqrt{(\omega^2 - \omega_0^2)^2 + 2n\omega}$, $\omega_0 = \frac{k_Z}{m_Z}$, $n = \frac{c_Z}{m_Z}$.

Generally, Eq. (9) can be used directly when the frequency is constant. If the frequency varies, the solution of Eq. (8) can also be obtained similarly as long as $f = f(t)$ can be determined. The solution can be used in dynamic analysis and design of control law.

The experimental and numerical result of GMA driving system when $f = 80$Hz was shown in Fig. 5, where triangular wave was used in testing the credibility of model (4). The amplitude of GMA in oscillograph was shown in real line, and numerical solution of Eq. (8) was shown in dashed line. We can see that the numerical solution of Eq. (8) is accord with experiment results from Fig. 5.

4. Conclusion

In this paper, a kind of giant magnetostrictive actuator model based on hysteretic nonlinear theory was developed. Nonlinear difference item was introduced to interpret the hysteresis phenomenon of GMM.

The coupling relationship between magnetic field intensity and frequency was obtained in stepwise multiple regression method. The new relationship among strain, magnetic field intensity and frequency can interpret the driftage of strain curve well, and the result of significance test shows that the effects of all of the items in the final model are remarkable. Based on above, the dynamic model of GMA was developed, and the numerical solution is accord with experiment result, which means that the new model can describe the characteristics of GMA in different frequencies well. The new GMA model broadens the region of controlling frequency, and is easy to be analyzed in theory, which is helpful to vibration control.

Acknowledgements

The authors gratefully acknowledge the support of Natural Science Foundation of China (NSFC) through grant no. 10732020 and the Ph.D. Programs Foundation of Ministry of Education of China through grant no. 200800561083.

References

[1] D.C. Jiles and D.L. Atherton, Theory of ferromagnetic hysteresis, *Journal of Magnetism and Magnetic Materials* **61** (1986), 48–60.
[2] J.B. Restorff, H.T. Savage and A.E. Clark, Preisach modeling of hysteresis in Terfenol-D, *Journal of Applied Physics* **67** (1990), 5016–5018.
[3] G.P. Carman and M. Mitrovic, Nonlinear constitutive relations for magnetostrictive materials with applications to 1-D problems, *Journal of Intelligent Materials System and Structure* **6** (1995), 673–684.
[4] F.T. Calkins, R.C. Smith and A.B. Flatau, Energy-based Hysteresis Model for Magnetostrictive Transducers, *IEEE Transactions on Magnetics* **36** (2000), 429–439.
[5] H.M. Zhou, Y.H. Zhou and X.J. Zheng, Numerical simulation of nonlinear dynamic responses of beams laminated with giant magnetostrictive actuators, *Computers Materials and Continua* **6** (2007), 201–211.
[6] L. Sun and X.J. Zheng, Numerical simulation on coupling behavior of Terfenol-D rods, *International Journal of Solids and Structures* **43** (2006), 1613–1623.
[7] R.G. Yan, B.W. Wang and Q.X. Yang, A numerical model of displacement for giant magnetostrictive actuator, *IEEE Transactions on Applied Superconductivity* **14** (2004), 1914–1917.
[8] S. Chakraborty and G.R. Tomlinson, An initial experiment into the change in magnetic induction of a Terfenol-D rod due to external stress, *Smart Structures and Materials* **12** (2003), 763–768.